# Non-Abelian Optical Lattices: Anomalous Quantum Hall Effect and Dirac Fermions

N. Goldman,[1] A. Kubasiak,[2,3] A. Bermudez,[4] P. Gaspard,[1] M. Lewenstein,[2,5] and M. A. Martin-Delgado[4]

[1]*Center for Nonlinear Phenomena and Complex Systems - Université Libre de Bruxelles (U.L.B.),
Code Postal 231, Campus Plaine, B-1050 Brussels, Belgium*
[2]*ICFO-Institut de Ciències Fotòniques, Parc Mediterrani de la Tecnologia, E-08860 Castelldefels (Barcelona), Spain*
[3]*Marian Smoluchowski Institute of Physics Jagiellonian University, Reymonta 4, 30059 Kraków, Poland*
[4]*Departamento de Física Teórica I, Universidad Complutense, 28040 Madrid, Spain*
[5]*ICREA - Instituciò Catalana de Ricerca i Estudis Avançats, 08010 Barcelona, Spain*
(Received 16 March 2009; revised manuscript received 29 May 2009; published 14 July 2009)

We study the properties of an ultracold Fermi gas loaded in an optical square lattice and subjected to an external and classical non-Abelian gauge field. We show that this system can be exploited as an optical analogue of relativistic quantum electrodynamics, offering a remarkable route to access the exotic properties of massless Dirac fermions with cold atoms experiments. In particular, we show that the underlying Minkowski space-time can also be modified, reaching anisotropic regimes where a remarkable anomalous quantum Hall effect and a squeezed Landau vacuum could be observed.

Low-energy excitations of fermionic lattice systems are usually governed by the nonrelativistic Schrödinger equation. However, this description must be profoundly altered in the vicinity of Dirac points, where the energy bands display conical singularities and quasiparticles become massless relativistic fermions. Such a remarkable behavior can be induced by a honeycomb geometry [1–5], or by additional uniform [6] or staggered [7,8] magnetic fields. Here, we show that the natural playground for emerging Dirac fermions is provided by multicomponent fermionic atoms subjected to artificial non-Abelian gauge fields. We emphasize that these external fields can be produced by generalizing the recent experiment [9], as proposed in [10,11]. Such gauge fields give rise to intriguing phenomena such as the non-Abelian Aharonov-Bohm effect [10], generation of magnetic monopoles [12], non-Abelian atom optics [13], quasirelativistic effects [14], or even the modification of the metal-insulator transition [15]. In this Letter, we show that the physical properties of massless relativistic fermions are completely characterized by the non-Abelian features of the external gauge fields. Furthermore, the anisotropy of the underlying Minkowski space-time can be controlled externally, producing an anomalous quantum Hall effect characterized by a squeezed Landau vacuum.

We consider a system of two-component (two-color) fermionic atoms trapped in an optical square lattice with sites at $\mathbf{r} = (n, m)a$, where $a$ is the lattice spacing and $n$, $m \in \mathbb{Z}$. In the noninteracting limit, which can be obtained by means of Feshbach resonances [16], fermions freely hop between neighboring sites. The addition of an external gauge potential $\mathbf{A}$ modifies the hopping Hamiltonian according to the Peierls substitution

$$H = -t \sum_{\langle \mathbf{r}, \mathbf{r}' \rangle} \sum_{\tau \tau'} c_{\tau'}^{\dagger}(\mathbf{r}') e^{-i \int_{\mathbf{r}}^{\mathbf{r}'} \mathbf{A} \cdot d\mathbf{l}} c_{\tau}(\mathbf{r}) + \text{H.c.}, \quad (1)$$

where $t$ is the hopping amplitude, $c_{\tau}(\mathbf{r})$ is the fermionic field operator in color component $\tau = 1, 2$, and we set $\hbar = e = 1$. Our setup features an external gauge potential with both commutative and noncommutative components $\mathbf{A} = \frac{B_0}{2}(-y, x) + a(B_{\alpha} \sigma_y, B_{\beta} \sigma_x)$, where $B_0$, $B_{\alpha}$, $B_{\beta}$ are controllable parameters and $\sigma_{x,y}$ are Pauli matrices. Accordingly, the hoppings are accompanied by nontrivial unitary operators, $U_x(m) = e^{-i\pi\Phi m} e^{i\Phi_{\alpha} \sigma_y}$ and $U_y(n) = e^{i\pi\Phi n} e^{i\Phi_{\beta} \sigma_x}$, where $\Phi = B_0 a^2$ is the Abelian magnetic flux and $\Phi_{\alpha,\beta} = B_{\alpha,\beta} a^2$ are the non-Abelian fluxes [see Fig. 1(a)].

Let us point out that the gauge fields considered in this work can be realized following the proposals [10,11,17], along the lines of the recent experiment [9], and provide non-Abelian analogues of homogeneous magnetic fields since they are characterized by constant Wilson loops. Indeed, atoms hopping around an elementary plaquette undergo a unitary transformation $U = U_x(m)U_y(n + 1)U_x^{\dagger}(m + 1)U_y^{\dagger}(n)$, explicitly given by
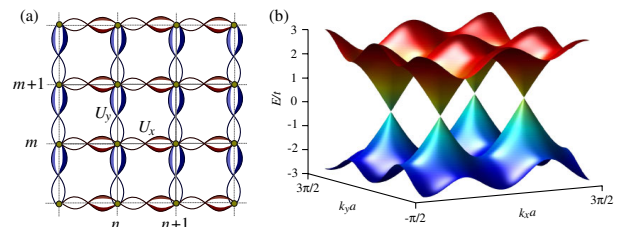


FIG. 1 (color online). (a) Square lattice subjected to a non-Abelian gauge potential. This external field induces state-dependent hoppings described by the U(2) operators $U_x$ and $U_y$. (b) Energy bands close to the $\pi$-flux regime ($\Phi_{\alpha} = \pi/2 + 0.1$, $\Phi_{\beta} = \pi/2 - 0.1$), with vanishing Abelian flux $\Phi = 0$. The bands touch at four Dirac points inside the first Brillouin zone (BZ), where the energy scales linearly with momenta $E \sim k$.

$$U = e^{i2\pi\Phi}(c_1\mathbb{1} + c_2\sigma_z + c_3\sigma_y + c_4\sigma_x), \qquad (2)$$

where the constants $\{c_j\}$ are listed in [18]. For specific values of $\Phi_{\alpha,\beta}$, the loop matrix reduces to a phase factor and reproduces the Abelian $\pi$-flux ($\Phi_\alpha = \Phi_\beta = \frac{\pi}{2}$) or Hofstadter ($\Phi_\alpha = \Phi_\beta = 0$) models [6,19]. However, in general cases, it is a nontrivial U(2) operator exhibiting non-Abelian properties such as the non-Abelian Aharonov-Bohm effect. The gauge-invariant Wilson loop $W = \mathrm{tr}U$ provides a clear distinction between the Abelian ($|W| = 2$) and non-Abelian ($|W| < 2$) regimes. We stress that the Wilson loop is homogeneous and that the corresponding spectrum exhibits well developed gaps [17].

In order to isolate non-Abelian effects, we first study the regime of vanishing Abelian flux $\Phi = 0$. The Hamiltonian is diagonalized in momentum space, and the fermion gas becomes a collection of noninteracting quasiparticles with energies shown in Fig. 1(b). Close to the marginally Abelian regime ($\Phi_\alpha$, $\Phi_\beta \approx \pi/2$), the spectrum develops four independent conical singularities $\mathbf{k}_D \in \{(0,0), (\frac{\pi}{a},0), (0,\frac{\pi}{a}), (\frac{\pi}{a},\frac{\pi}{a})\} \in$ BZ, which correspond to massless relativistic excitations at half filling. Around these points $\mathbf{p} = \mathbf{k} - \mathbf{k}_D$, the low-energy properties are accurately described by a Dirac Hamiltonian

$$H_{\mathrm{eff}} = \sum_{\mathbf{p}}\Psi_{\mathbf{p}}^\dagger H_D \Psi_{\mathbf{p}}, \qquad H_D = c_x\alpha_x p_x + c_y\alpha_y p_y, \quad (3)$$

where $\Psi_{\mathbf{p}} = (c_{1\mathbf{p}}, c_{2\mathbf{p}})^t$ is the relativistic spinor, the Dirac matrices $\alpha_x$, $\alpha_y$ fulfill $\{\alpha_j, \alpha_k\} = 2\delta_{jk}$ [e.g., around $\mathbf{k}_D = (0, \pi/a)$, $\alpha_x = \sigma_y$, and $\alpha_y = \sigma_x$], and $c_x = 2at\sin\Phi_\alpha$, $c_y = 2at\sin\Phi_\beta$ represent the effective speed of light. We stress here that the control over the non-Abelian fluxes $\Phi_{\alpha,\beta}$ offers the exotic opportunity to modify the structure of the underlying Minkowski space-time, reaching aniso-tropic situations where $c_x \neq c_y$. Hence, non-Abelian optical lattices provide a quantum optical analogue of relativistic QED, where the emerging fermions and the properties of the corresponding space-time rely on the non-Abelian features of the external fields. Furthermore, it is also possible to observe a transition between relativistic and nonrelativistic dispersion relations as the energy is increased. This abrupt change of the quasiparticle nature is revealed by Van Hove singularities (VHS) in the density of states, as displayed in Figs. 2(a) and 2(c).

The transport properties of 2D Fermi gases subjected to external gauge fields are characterized by the optical-lattice analogue of the well-known quantum Hall effect (QHE) [20]. In this context, the transverse Hall conductivity measures the response of the system to a static force, e.g., a lattice acceleration, and takes on quantized values $\sigma_{xy} = \frac{\nu}{h}$ with $\nu \in \mathbb{Z}$, when the Fermi energy $E_F$ lies in a gap [17]. Surprisingly, the quantized conductivity of cold gases can be directly observed through density measurements thanks to the Streda formula [21]. Here, we show that non-Abelian effects have dramatic consequences on the QHE which occurs when an additional Abelian flux $\Phi$
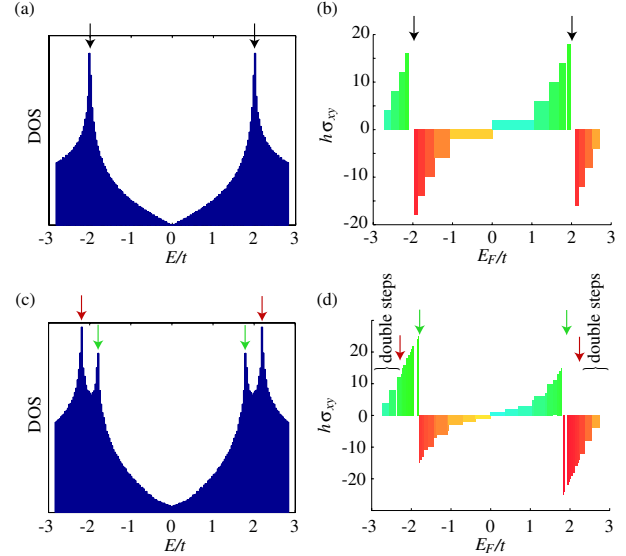


FIG. 2 (color online).    (a) Density of states (DOS) in the $\pi$-flux regime $\Phi_\alpha = \Phi_\beta = \pi/2$ when $\Phi = 0$. (b) Hall conductivity in units of $h^{-1}$ as a function of the Fermi energy in the same regime for $\Phi = 1/41$. Black arrows designate the VHS. (c) DOS close to the $\pi$-flux regime $\Phi_\alpha = \pi/2 + 0.1$ and $\Phi_\beta = \pi/2 - 0.1$ when $\Phi = 0$. (d) Hall conductivity $h\sigma_{xy} = h\sigma_{xy}(E_F)$ in the same regime as (c) for $\Phi = 1/41$. Dark red and light green arrows, respectively, designate the VHS $E_{\mathrm{red}}^{\mathrm{VHS}}$ and $E_{\mathrm{green}}^{\mathrm{VHS}}$ [cf. Eq. (6)].

is applied to our system. The quantized values of the transverse conductivity are calculated as the sum of topo-logical invariants associated to each energy band, the so-called Chern numbers [22],

$$\sigma_{xy} = -\sum_{E_n < E_F}\frac{i}{2\pi h}\int_{\mathrm{BZ}}\mathrm{tr}\mathcal{F}(\psi_n)\mathbf{dk}, \qquad (4)$$

where $\mathcal{F}(\psi_n) = \langle\partial_{k_x}\psi_n|\partial_{k_y}\psi_n\rangle - \langle\partial_{k_y}\psi_n|\partial_{k_x}\psi_n\rangle$ is the Berry's curvature of the band $E_n$. Here, the Chern numbers are computed numerically by discretizing the Brillouin zone [23]. A lattice gauge theory method allows to deter-mine the Berry's curvature

$$\mathcal{F}_{xy}(\boldsymbol{k}_l) = \ln T_x(\boldsymbol{k}_l)T_y(\boldsymbol{k}_l + \hat{\boldsymbol{x}})T_x(\boldsymbol{k}_l + \hat{\boldsymbol{y}})^{-1}T_y(\boldsymbol{k}_l)^{-1},$$
$$T_\mu(\boldsymbol{k}_l) = \langle\psi_n(\boldsymbol{k}_l)|\psi_n(\boldsymbol{k}_l + \hat{\boldsymbol{\mu}})\rangle, \qquad (5)$$

and subsequently the Chern number $C = \frac{i}{2\pi}\sum_l\mathcal{F}_{xy}(\boldsymbol{k}_l)$. Remarkably, the sequence of Hall plateaus is extremely sensitive to the values of the non-Abelian fluxes. In the Abelian regime $\Phi_\alpha = \Phi_\beta = 0$, we observe that the Hall conductivity follows the usual integer QHE $\sigma_{xy} = \frac{2\nu}{h}$, where the factor 2 is due to color-degeneracy. Conversely, in the $\pi$-flux regime ($\Phi_\alpha = \Phi_\beta = \pi/2$) illus-trated in Fig. 2(b), we obtain a completely different se-quence of Hall plateaus where $\sigma_{xy} = \frac{4}{h}(\nu + \frac{1}{2})$ around $E_F = 0$, as recently observed in graphene [4]. This se-quence is characterized by sudden changes of sign across the VHS situated at $E = \pm 2$, and by unusual double steps

which can be traced back to the underlying low-energy relativistic excitations. As the gauge fluxes vary in the vicinity of the $\pi$-flux point ($\Phi_\alpha = \pi/2 + \epsilon$ and $\Phi_\beta = \pi/2 - \epsilon$), the system enters the non-Abelian regime and the Hall plateaus are modified [see Fig. 2(d)]. Indeed, most of the degeneracies induced by the Dirac points are lifted, and the anomalous double steps around $E_F = 0$ are progressively destroyed. However, a striking behavior occurs: as the non-Abelian fluxes are varied, the two VHS originally situated at $E = \pm 2$ in the $\pi$-flux point are split into four

$$E_{\text{red}}^{\text{VHS}} = \pm 2(1 + \cos\Phi_\beta), \quad E_{\text{green}}^{\text{VHD}} = \pm 2(1 + \cos\Phi_\alpha), \quad (6)$$

as illustrated in Fig. 2(c) for $\epsilon = 0.1$. Surprisingly enough, anomalous double steps in the plateau sequence reappear at higher energies outside the two *red* VHS, while the *green* VHS induce a sudden change of sign [see Figs. 2(c) and 2(d)]. It is interesting to note that the anomalous behavior persists in the high-energy regime and that this effect can be probed by varying the parameter $\Phi_\beta$. The temperature required to observe these plateaus should be smaller than the spectral gaps, namely $T \sim 10$ nK.

To identify the non-Abelian features in this QHE, we introduce the Abelian flux $\Phi$ in the Dirac Hamiltonian (3) by minimal coupling $\mathbf{p} \rightarrow \mathbf{p} + \frac{B_0}{2}(-y, x)$, and obtain

$$H_D = (g_-\sigma^+ a + g_-\sigma^- a^\dagger) + (g_+\sigma^+ a^\dagger + g_+\sigma^- a), \quad (7)$$

where $\sigma^+ = |\chi_1\rangle\langle\chi_2|$, $\sigma^- = |\chi_2\rangle\langle\chi_1|$ are color-flip operators, $g_\pm = (c_y \pm c_x)(B_0/2)^{1/2}$, and $a^\dagger$, $a$ are bosonic chiral operators listed in [24]. In the isotropic limit $g_- = 0$, the Hamiltonian consists of an anti-Jaynes-Cummings term, a well-known interaction in quantum optics [25] that leads to the usual relativistic Landau levels (LL) recently observed in graphene [2]. Conversely, in the non-Abelian regime $g_- \neq 0$, the Hamiltonian becomes a simultaneous combination of Jaynes-Cummings and anti-Jaynes-Cummings terms, producing a new type of Landau levels. These novel LL are obtained by means of a Bogoliubov squeezing transformation $S(\zeta) = e^{\zeta/2[a^2 - (a^\dagger)^2]}$ with $\zeta = -\tanh^{-1}(g_-/g_+)$, leading to the energy spectrum

$$E_{\text{LLL}} = 0, \quad E_n^\pm = \pm\sqrt{(2B_0c_xc_y)n}, \quad n = 1, 2\ldots \quad (8)$$

and corresponding eigenstates

$$|\text{LLL}\rangle = |\chi_2\rangle S^\dagger(\zeta)|\text{vac}\rangle,$$
$$|E_n^\pm\rangle = \frac{1}{\sqrt{2}}|\chi_1\rangle S^\dagger(\zeta)|n-1\rangle \pm \frac{1}{\sqrt{2}}|\chi_2\rangle S^\dagger(\zeta)|n\rangle, \quad (9)$$

with $|n\rangle = (n!)^{-1/2}(a^\dagger)^n|\text{vac}\rangle$ being the usual Fock states. Accordingly, the effect of non-Abelian fields is to squeeze the usual LL. In particular, the lowest Landau level (LLL) is a zero-energy mode characterized by a colored squeezed vacuum, which is in clear contrast with its Abelian counterpart, the latter being simply the vacuum. Besides, this LLL

presents half the degeneracy of the remaining excited states $n \geq 1$ [26], and leads to the so-called anomalous half-integer QHE

$$\sigma_{xy} = \pm\frac{g}{h}\left(\nu + \frac{1}{2}\right), \quad (10)$$

where the filling factor $\nu$ is defined as the integer part of $[E_F^2/2B_0c_xc_y]$, and $g$ is the Dirac points degeneracy. Let us stress that the non-Abelian fluxes modify the Hall plateaus in a nontrivial manner as already emphasized through the numerical results. In particular, the Hall conductivity in Eq. (10) predicts the anomalous half-integer plateaus represented in Fig. 2(b), where the conical singularities are four-fold degenerate $g = 4$. Conversely, in the non-Abelian case shown in Fig. 2(d), the degeneracy is lifted to $g = 1$, and thus the size of the steps is modified in accordance.

As discussed above, the anomalous QHE is essentially a single-particle phenomenon that relies on the peculiar properties of the LLL. Additionally, further non-Abelian anomalies can also be found at the many-particle level, where an exotic Laughlin wave function [27] can be obtained by filling the single-particle vortex wave functions

$$\phi_{\text{LLL}}^m(x, y) = \left(\sqrt{\frac{c_y}{c_x}}x - i\sqrt{\frac{c_x}{c_y}}y\right)^m e^{-(x^2/2\tau_x^2 + y^2/2\tau_y^2)}. \quad (11)$$

Here, $\tau_x = l_B\sqrt{2c_x/c_y}$, $\tau_y = l_B\sqrt{2c_y/c_x}$, describe the anisotropic extent of the wave function in units of the magnetic length $l_B = \sqrt{1/B_0}$, and $m = 0, 1\ldots$ represents the number of left-handed quanta [24]. Note how the loss of rotational invariance caused by the non-Abelian induced anisotropy $c_x \neq c_y$, leads to the squeezing of the vortex levels [Figs. 3(a)–3(d)]. Filling these squeezed degenerate states (11) according to Fermi statistics, we obtain the Laughlin wave function



(a) Nonsqueezed wave function    (b) Isotropic section

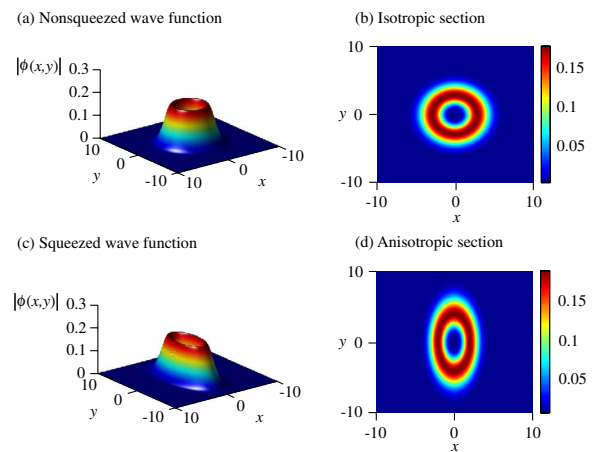(c) Squeezed wave function    (d) Anisotropic section

FIG. 3 (color online). Vortex-like single-particle wave functions of the LLL $\phi_{\text{LLL}}^m(x, y)$ for $m = 4$. (a), (b) Isotropic limit $c_x = c_y$. (c), (d) Anisotropic regime $c_y = 2c_x$. Note that distances are measured in units of the magnetic length $l_B$.

$$\Psi[z] = \prod_{j<k}(u z_{jk} - v \bar{z}_{jk})e^{-\sum_j f(u,v)|z_j|^2 - g(u,v)(z_j^2 + \bar{z}_j^2)}, \quad (12)$$

where $u = \cosh\zeta$, $v = \sinh\zeta$, $f(u,v) = \frac{1}{4}(u^2 + v^2)$, and $g(u,v) = \frac{1}{4}uv$ depend on the anisotropy through the squeezing parameter $\zeta$, and $z_{jk} = z_j - z_k$ represents the complex two-fermion distance. In the Abelian limit $\zeta = 0$, one recovers the standard integer Laughlin wave function $\Psi[z] = \prod_{j<k}f(z_j, z_k)e^{-\sum_j |z_j|^2/4l_B^2}$, where $f(z_j, z_k) = z_j - z_k$ belongs to the space of holomorphic functions (Bargman-Fock space [28]). Strikingly, in the non-Abelian scenario $\zeta \neq 0$, the wave function (12) does not belong to such space due to the interference between holomorphic $f(z)$ and antiholomorphic $f(\bar{z})$ components, and thus represents an instance of a nonchiral QHE. As shown below, this new anomaly modifies the classical analogy with the one-component plasma (OCP), the building block that characterizes the peculiar properties of quasiparticles in the fractional QHE [20]. The Laughlin state can be interpreted as the partition function of a OCP $|\Psi[z]|^2 \propto Z_c = \int \prod_j dz_j d\bar{z}_j e^{-U_c/kT}$ with $kT = 1/2$, a classical gas of particles interacting with a charged background through the potential

$$U_c = -\sum_{jk}\log|u z_{jk} - v \bar{z}_{jk}| + \frac{1}{4}\sum_j [f|z_j|^2 - g(z_j^2 + \bar{z}_j^2)]. \quad (13)$$

The last term corresponds to the charged background jellium $\rho_j = -\frac{1}{4\pi l_B^2}\left(\frac{c_x}{c_y} + \frac{c_y}{c_x}\right)$, whereas the first describes a collection of positively charged particles $q = 1$ surrounded by a charge cloud $\delta\rho(z)$, with $z = |z|e^{-i\theta}$, and

$$\delta\rho(|z|, \theta) = \frac{\tanh\zeta}{|z|^2}\frac{(1 + \tanh^2\zeta)\cos 2\theta - 4\tanh\zeta}{(1 + \tanh^2\zeta) - 4\tanh\zeta\cos 2\theta}. \quad (14)$$

Notice how the surrounding charge cloud is absent $\delta\rho(z) = 0$ in the Abelian limit $\zeta = 0$, and we recover the usual OCP analogy. Conversely, for non-Abelian regimes, the collection of interacting positively charged particles becomes locally surrounded by an anisotropic charge cloud $\rho = \sum_j q\delta(z - z_j) + \delta\rho(z_j)$ with $\int d^2z\delta\rho(z) = 0$. In accordance, the paradigmatic plasma analogy is altered due to the squeezed nature of the LLL, a fact that may find profound consequences in the fractional QHE.

We have shown that non-Abelian optical lattices offer an intriguing route to probe the striking properties of emerging Dirac fermions in anisotropic Minkowski space-times. In particular, the versatility offered by such experimental setups leads to the unique possibility of tuning the anisotropy of the underlying space-time, leading to remarkable effects such as nonchiral quantum Hall effects with several types of anomalies.

[1] G. W. Semenoff, Phys. Rev. Lett. **53**, 2449 (1984).

[2] A. H. Castro Neto, F. Guinea, N. M. R. Peres, K. S. Novoselov, and A. K. Geim, Rev. Mod. Phys. **81**, 109 (2009).

[3] K. S. Novoselov et al., Nature (London) **438**, 197 (2005).

[4] Y. B. Zhang, Y. W. Tan, H. L. Stormer, and P. Kim, Nature (London) **438**, 201 (2005).

[5] S.-L. Zhu, B. Wang, and L.-M. Duan, Phys. Rev. Lett. **98**, 260402 (2007).

[6] X. G. Wen, Quantum Field Theory of Many-Body Systems (Oxford Univ. Press, Oxford, 2004).

[7] L.-K. Lim, C. M. Smith, and A. Hemmerich, Phys. Rev. Lett. **100**, 130402 (2008).

[8] J.-M. Hou, W.-X. Yang, and X.-J. Liu, Phys. Rev. A **79**, 043621 (2009).

[9] Y.-J. Lin et al., Phys. Rev. Lett. **102**, 130401 (2009).

[10] K. Osterloh, M. Baig, L. Santos, P. Zoller, and M. Lewenstein, Phys. Rev. Lett. **95**, 010403 (2005).

[11] J. Ruseckas, G. Juzeliunas, P. Öhberg, and M. Fleischhauer, Phys. Rev. Lett. **95**, 010404 (2005).

[12] V. Pietilä and M. Möttönen, Phys. Rev. Lett. **102**, 080403 (2009).

[13] G. Juzeliūnas, J. Ruseckas, A. Jacob, L. Santos, and P. Öhberg, Phys. Rev. Lett. **100**, 200405 (2008).

[14] G. Juzeliūnas, J. Ruseckas, M. Lindberg, L. Santos, and P. Öhberg, Phys. Rev. A **77**, 011802(R) (2008).

[15] I. I. Satija, D. C. Dakin, and C. W. Clark, Phys. Rev. Lett. **97**, 216401 (2006).

[16] I. Bloch, J. Dalibard, and W. Zwerger, Rev. Mod. Phys. **80**, 885 (2008).

[17] N. Goldman, A. Kubasiak, P. Gaspard, and M. Lewenstein, Phys. Rev. A **79**, 023624 (2009).

[18] $c_1 = \cos^2\Phi_\alpha + \cos 2\Phi_\beta \sin^2\Phi_\alpha$, $c_2 = \frac{i}{2}\sin 2\Phi_\alpha \sin 2\Phi_\beta$, $c_3 = i\sin 2\Phi_\alpha \sin^2\Phi_\beta$, $c_4 = -i\sin^2\Phi_\alpha \sin 2\Phi_\beta$.

[19] R. Hofstadter, Phys. Rev. B **14**, 2239 (1976).

[20] M. Stone, Quantum Hall Effect (World Scientific, London, 1992).

[21] R. O. Umucalilar, H. Zhai, and M. Ö. Oktel, Phys. Rev. Lett. **100**, 070402 (2008).

[22] M. Kohmoto, Ann. Phys. (N.Y.) **160**, 343 (1985).

[23] T. Fukui, Y. Hatsugai, and H. Suzuki, J. Phys. Soc. Jpn. **74**, 1674 (2005).

[24] Right-handed $a = (a_x - ia_y)/\sqrt{2}$ and left-handed $b = (a_x + ia_y)/\sqrt{2}$ operators are defined in terms of the usual Cartesian modes $a_j = \sqrt{\frac{\omega}{2}}(x_j + \frac{i}{\omega}p_j)$, where $\omega = B_0/2$.

[25] E. T. Jaynes and F. W. Cummings, Proc. IEEE **51**, 89 (1963).

[26] V. P. Gusynin and S. G. Sharapov, Phys. Rev. Lett. **95**, 146801 (2005).

[27] R. B. Laughlin, Phys. Rev. Lett. **50**, 1395 (1983).

[28] S. M. Girvin and T. Jach, Phys. Rev. B **29**, 5617 (1984).